

On Hurricane Outflow Structure

CHUN-CHIEH WU* AND KERRY A. EMANUEL

Center for Meteorology and Physical Oceanography, Massachusetts Institute of Technology, Cambridge, Massachusetts

2 September 1993 and 17 December 1993

ABSTRACT

Flow fields from the model of Wu and Emanuel are presented. It is demonstrated that the interaction of background shear with a uniform source of low potential vorticity air at the storm top can produce many of the observed characteristics of hurricane outflow, including outflow jets. Our model is compared to other extant models of hurricane outflow.

1. Introduction

Observations show that tropical cyclones are strongly baroclinic, with broad anticyclones aloft. These storms are typically embedded in a large-scale potential vorticity gradient that is highly inhomogeneous. These properties may substantially influence the movement and structure of such storms.

Wu and Emanuel (1993, hereafter WEM) have noted that the anticyclone above a hurricane may interact with the lower hurricane vortex and induce storm motion. Such interaction can be caused by both the direct effect of the ambient vertical shear and the effect of the vertical variation of the background potential vorticity gradient. To isolate the direct effect of vertical wind shear on the motion of a baroclinic vortex, WEM conducted experiments with an idealized two-layer quasigeostrophic model in which there is no background potential vorticity gradient, motivated in part by the observation that such gradients are very weak in the interior of the troposphere.

WEM found that the direct effect of ambient vertical shear is to displace the upper-level plume of anticyclonic relative potential vorticity downshear from the lower-layer cyclonic point potential vortex, thus inducing a mutual interaction between the circulations associated with each potential vorticity anomaly. This results in a drift of the point vortex broadly to the left of the vertical shear vector (in the Northern Hemisphere). The magnitude of this drift is generally com-

parable to that found in simulations of barotropic vortices on the β plane.

The hurricane outflow is the outward branch of the hurricane's circulation in the upper troposphere. Observations from both the case study of Black and Anthes (1971) and the composite study of Merrill (1988) showed that the outflow is quite asymmetric. It often contains one or two anticyclonically curved outflow jets with different preferential patterns, depending on the types of synoptic-scale features they interact with. This kind of asymmetric outflow structure has also been produced above a mature storm in three-dimensional numerical models (Anthes 1972; Kurihara and Tuleya 1974). Recently Ooyama (1987) employed a simple two-dimensional numerical model integrating the shallow water equations with specified sources of mass and momentum to simulate the effects of hurricane outflow. He showed that asymmetric jetlike outflow patterns can be generated in environments with horizontal shear.

It has been suggested that the evolution of the hurricane outflow plays important roles in influencing both the storm motion (WEM; Flatau and Stevens 1993) and hurricane structure change (Holland and Merrill 1984). The outflow also provides a channel that carries high potential temperature air from the convective core region outward to the far environment, where the air is cooled by radiation. From the standpoint of energetics, this is an important process that completes one branch of the hurricane Carnot cycle (Emanuel 1986).

Here we present wind fields produced by the model described in WEM and show that several well-known features of hurricane outflow structure are reproduced.

2. Background of the model

The approach taken in WEM is to simulate the interaction of a baroclinic vortex dipole with the back-

* Current affiliation: Program in Atmospheric and Oceanic Sciences, Princeton University, Princeton, New Jersey.

Corresponding author address: Dr. Chun-Chieh Wu, Geophysical Fluid Dynamics Laboratory, Princeton University, Forrestal Campus, US Route 1, P.O. Box 308, Princeton, NJ 08542.

ground shear, using the methods of contour dynamics and contour surgery to integrate the upper-level pseudopotential vorticity equation. A mature tropical cyclone is modeled as a diabatically and frictionally maintained point vortex of constant strength in the lower layer and, in the upper layer, a patch of uniform, zero potential vorticity (PV) air surrounded by an infinite region of constant potential vorticity.

The key assumption in such a model is that the diabatic sink of potential vorticity in the upper layer can be represented as the expansion of the area of the upper potential vorticity anomaly owing to a radial outward potential flow emanating from a point-mass source coinciding with the lower vortex. Physically, this representation mimics the action of moist convection near the hurricane center in creating a source of near-zero PV air in the upper troposphere, which is advected outward by the upper-level divergent hurricane outflow. The idealization of a patch of near-zero PV air in the upper troposphere is based both on the results from the numerical simulations of Rotunno and Emanuel (1987) and on the theoretical argument that the saturated moist potential vorticity is close to zero in a state of slantwise moist neutrality (the upper-tropospheric air is so cold and dry that the PV is very nearly equivalent to the saturated moist potential vorticity). Note that this idealization automatically accounts for momentum transports by cumulus convection. For a quasi-steady hurricane, the vertical mass flux is mainly controlled by Ekman pumping in the boundary layer. Therefore, according to the principle of mass continuity, the upper divergent potential flow can be derived from the lower boundary frictionally driven mass influx, as formulated in section 3e of WEM. To get a feeling for how this potential flow changes the real PV in the upper layer, here we also approximate the PV destruction rate in the model (shown in the appendix).

3. Outflow structure

In this section, we discuss the time evolution of the wind fields associated with the vorticity anomalies. These wind fields were not shown in WEM. The parameters described in this section are defined in the same way as in WEM. The initial wind distributions in each layer are shown in Fig. 1 for the control experiment, in which there is no background vertical shear (details of this experiment are described in WEM). It can be seen that the upper flow is cyclonic and outward with a maximum wind of about 3 m s^{-1} , and that the lower-layer flow is cyclonic with a maximum wind of about 28 m s^{-1} at the grid point closest to the point vortex. (The flow in the upper layer in this case consists of the rotational flow associated with the expanding zero PV patch, the imposed divergent flow, and the upward projection of the cyclonic flow in the lower layer. The flow in the lower layer consists of the flow

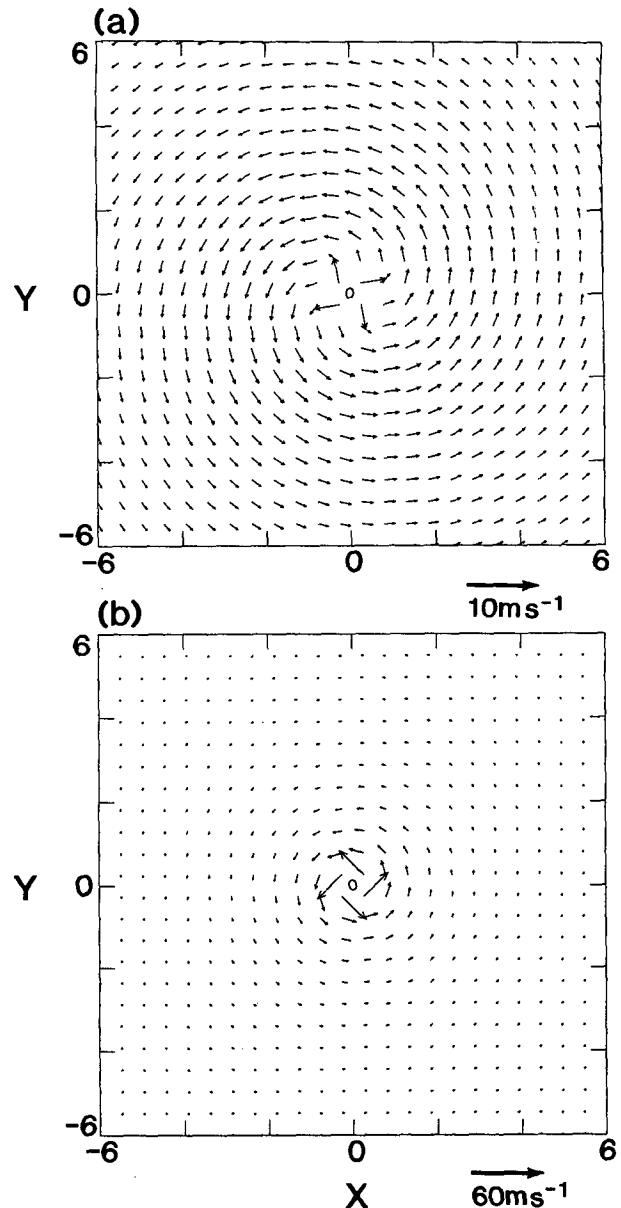


FIG. 1. (a) Initial upper-layer wind fields and (b) the initial lower-layer wind fields for $\epsilon = 0.25$, $\gamma = 0.79$, and $\chi = 0$. The lower vortex is located in the center and is shown as "O." One unit length in the domain corresponds to 500 km; ϵ , γ , and χ are defined in the same way as in WEM.

associated with the specified point vortex and the downward projection of the anticyclonic flow in the upper layer.) Figure 2 displays the evolution with time of the upper-layer flows for this case (note that Fig. 2d is identical to Fig. 3 of WEM). As the upper-layer vortex patch expands, the anticyclonic flow becomes stronger and covers a larger area. At t (dimensionless time) = 4, the maximum anticyclonic flow has increased to nearly 17 m s^{-1} . The evolution of lower-

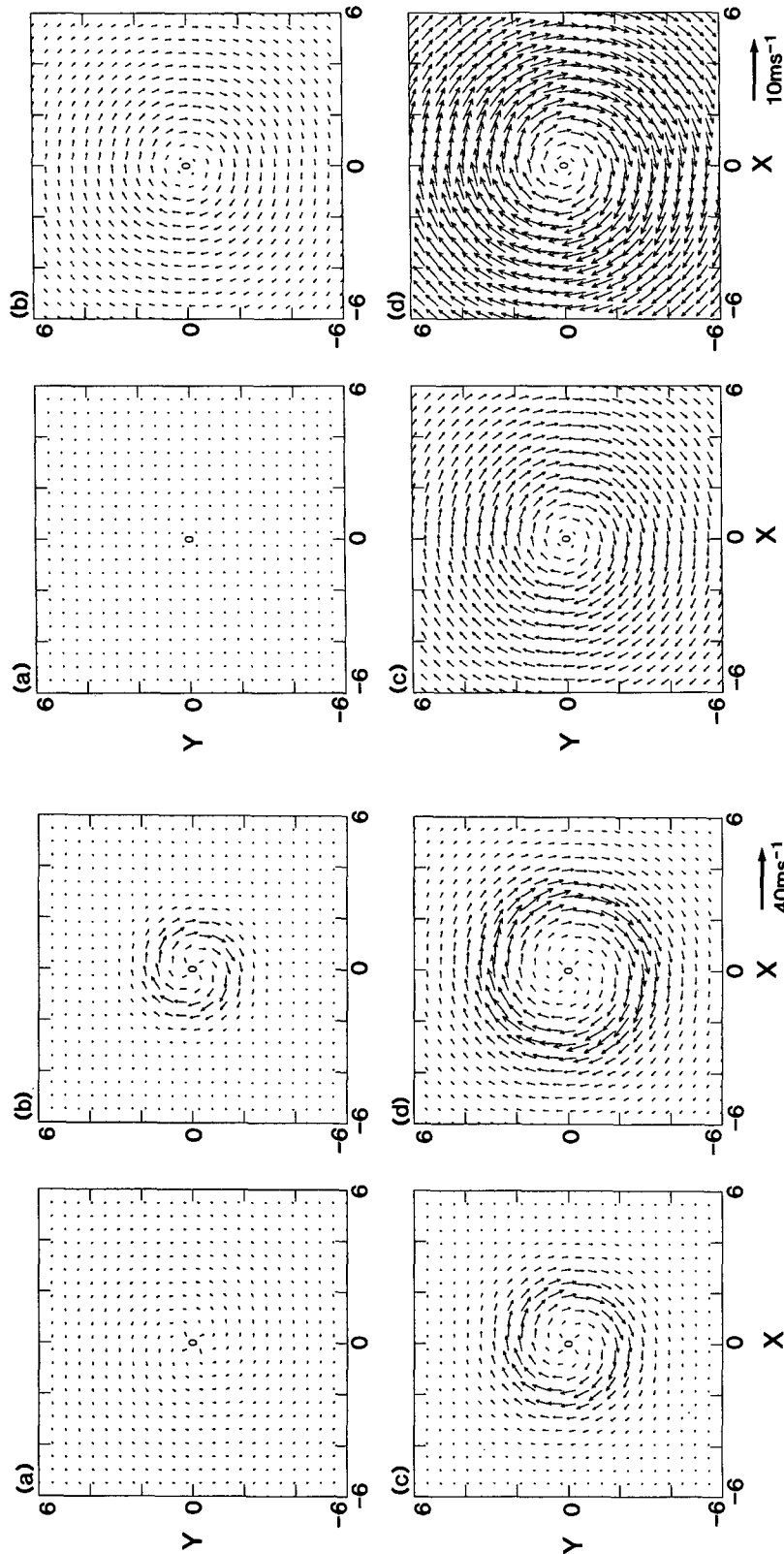


FIG. 2. Time evolution of the upper-layer wind fields for $\epsilon = 0.25$, $\gamma = 0.79$, and $X = 0$ at (a) $t = 0$, (b) $t = 1$, (c) $t = 2$, and (d) $t = 4$. The lower vortex is located in the center and is shown as "O." One unit length in the domain corresponds to 500 km.

FIG. 3. Time evolution of the lower-layer wind fields associated with the upper vortex patch for $\epsilon = 0.25$, $\gamma = 0.79$, and $X = 0$ at (a) $t = 0$, (b) $t = 1$, (c) $t = 2$, and (d) $t = 4$. The lower vortex is located in the center and is shown as "O." One unit length in the domain corresponds to 500 km.

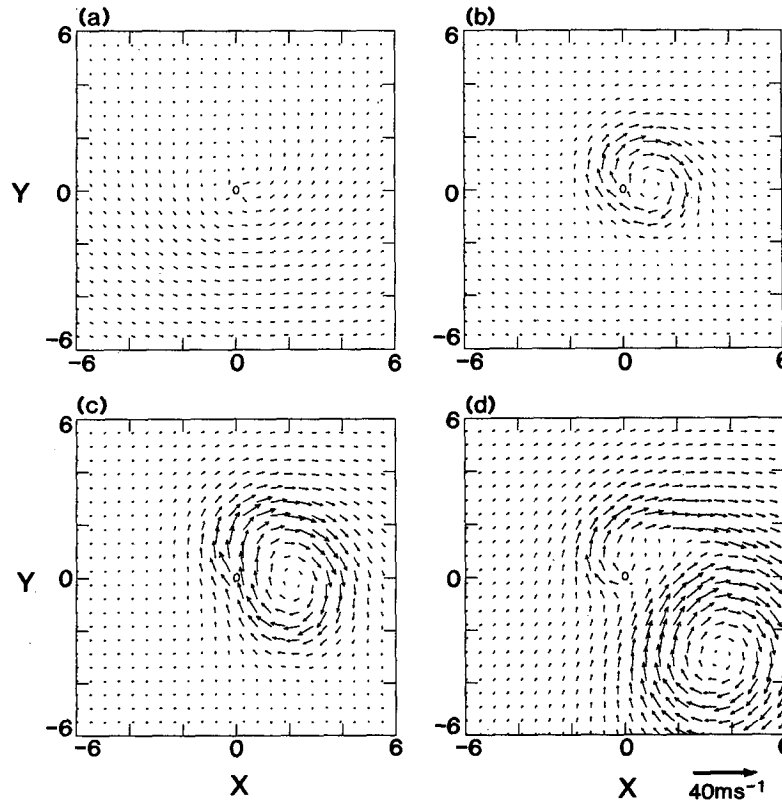


FIG. 4. As in Fig. 2 but for $\chi = 1.25$.

layer flow associated with the upper-layer vorticity patch (Fig. 3) indicates a weak, but strengthening anticyclonic flow symmetrically surrounding the vortex center, so that no vortex drift is induced. The total flow field in the lower layer (not shown) is similar to that of the initial condition (Fig. 1b), though it has a slightly weaker intensity because of the projection of the anticyclonic flow from the upper-layer vortex.

For the case with weak westerly shear [χ (nondimensional vertical shear) = 1.25], the time evolution of flow fields in the upper layer is shown in Fig. 4. The mean shear breaks the axisymmetry and advects the vorticity patch to the east (downshear), thus inducing southerly winds over the lower-layer vortex. After some time, the closed anticyclone breaks off and an outflow jet forms to the northeast.

Are such vorticity and flow fields realistic, or are they simply artifacts of the model? Figure 5 (from Molinari 1993) shows the time evolution of the upper-tropospheric PV and wind fields surrounding Hurricane Allen (1980). The mean vertical shear (averaged over the inner 500-km circle of Allen) between 800 and 200 mb calculated by Molinari (1993, personal communication) is weak and from the west-southwest at 0000 UTC 5 August 1980, then turns into a stronger west-southwesterly of about 7 m s^{-1} at 1200 UTC, and fi-

nally turns southwesterly at 0000 UTC 6 August. These observations clearly show an area of near-zero PV air above the downshear side of Hurricane Allen. A region of anticyclonic flow to the east of Hurricane Allen associated with the upper negative PV anomaly bears much resemblance to the flow field in our model (Fig. 4). This suggests that our idealized model does represent some features observed in real hurricanes. The lower-layer flow fields associated with the upper vortex patch (Fig. 6) indicate how this flow advects the lower-layer vortex. For example, at the end of model integration ($t = 4$), it contributes to nearly 3 m s^{-1} to a northward movement of the lower vortex.

For cases with very little shear, for example, $\chi = 0.25$, the upper vortex patch expands and rotates around the lower point vortex in time (Fig. 7). The balanced flow in the lower layer associated with the upper vortex patch is indicated in Fig. 8. It can be seen that near the end of the model integration, as the upper vortex patch drifts to the south, more eastward vortex drift is found.

For cases with larger westerly shear, for example, $\chi = 5$, the upper-layer flow fields (Fig. 9) indicate that an outflow jet exists to the northeast of the lower-layer vortex, and that the main anticyclonic flow is advected to the downshear side. The evolution of the lower-layer

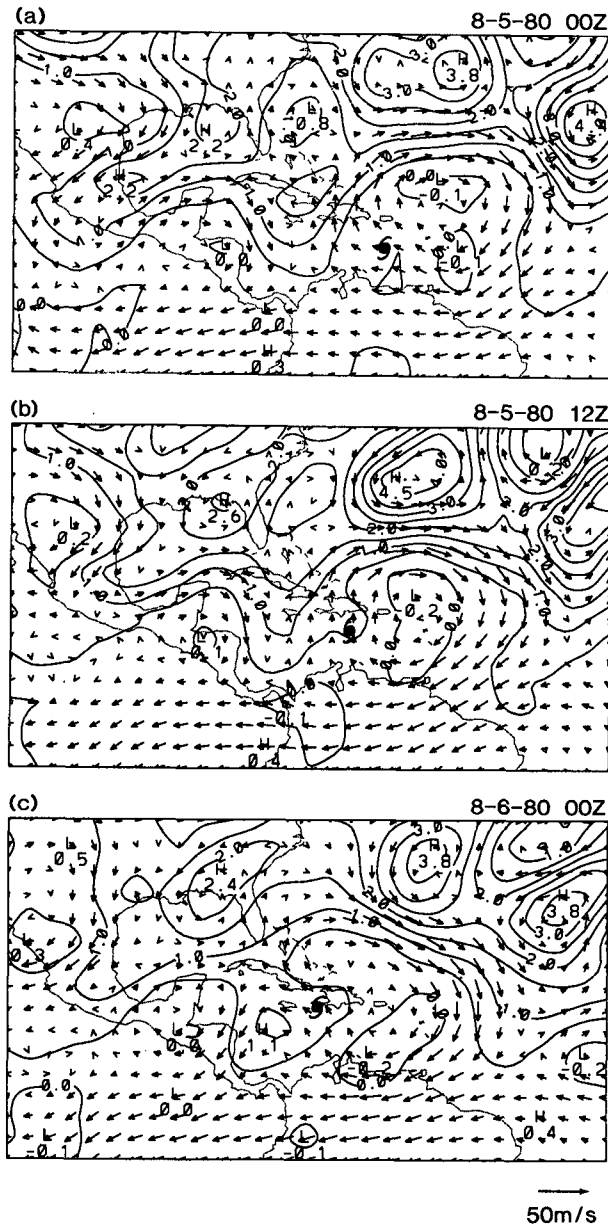


FIG. 5. Isentropic potential vorticity at 350 K at (a) 0000 UTC 5 August, (b) 1200 UTC 5 August, and (c) 0000 UTC 6 August 1980. The contour interval is 0.5 potential vorticity unit ($10^{-6} \text{ m}^2 \text{ s}^{-1} \text{ K kg}^{-1}$). Hurricane Allen is shown by the tropical storm symbol (Molinari 1993).

flow field associated with the upper vortex (Fig. 10) demonstrates that the influence of the upper vortex on the point vortex is to induce a consistent northwestward motion.

Combined with the results of WEM, the evolution of the wind field shown here clearly indicates that upper-tropospheric PV distributions, which are modified by both the synoptic-scale background flow and the upper

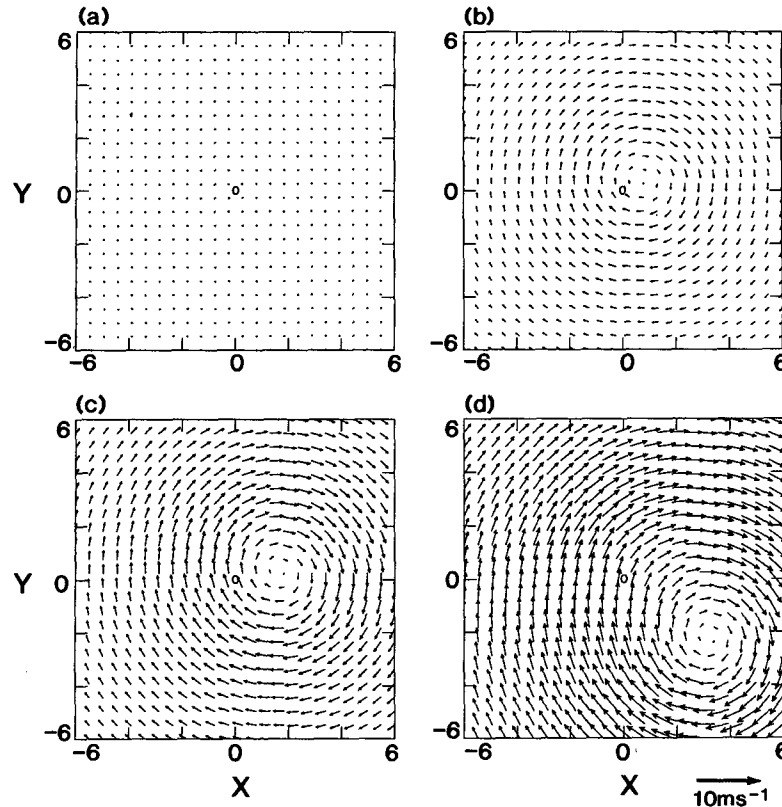
hurricane outflow itself, can be important in influencing storm motion and outflow structure. This result may have implications for the development of new observational platforms for improving the understanding and prediction of hurricane motion (Langford and Emanuel 1993).

Though the objectives of WEM and Ooyama (1987) are quite different, the two models are somewhat similar in the way in which outflow structure is created from the interaction of the divergent outflow with the mean environmental flow. In our case, the outflow structure is created through the interaction of zero PV outflow with an environment moving at a constant speed with respect to the outflow source, whereas in Ooyama's, the structure results from the interaction between outflow with an environment with specified horizontal shear. We argue that the PV view provides the simplest conceptual framework for understanding the dynamics of these interactions.

4. Summary

The dynamic properties of potential vorticity have been extensively utilized in observational work in meteorology after the thorough review by Hoskins et al. (1985). Here and in WEM we have attempted to show that potential vorticity concepts can be usefully applied to the understanding of hurricane movement and, to some extent, to hurricane structure, even though there exist strong sources of PV. In particular, the theory of slantwise moist convection and output from detailed numerical simulations suggest that hurricanes may be considered to be localized sources of nearly zero potential vorticity air in the upper troposphere. This concept entails a generalized notion of convective adjustment that includes the effect of cumulus momentum transport and leads to a clear conceptual picture of the interaction of hurricanes with their background flow. This picture, together with the simple numerical integrations presented here and in WEM, show that the interaction of the baroclinic hurricane vortex with background vertical shear may lead to storm drift, relative to the background mean flow, to the left (Northern Hemisphere) of the shear vector, and to a strong deformation of the outflow potential vorticity, resulting in jetlike outflow structure. These concepts have to be modified when background potential vorticity gradients are present (Shapiro 1992), though observations (e.g., Davis and Emanuel 1991; WEM) seem to suggest that potential vorticity is well mixed in the troposphere, at least in the middle latitudes and subtropics. We regard the characterization of the climatological distributions of potential vorticity as an important task in atmospheric science.

Acknowledgments. We thank Dr. John Molinari for helpful discussions. We also thank Dr. Lloyd Shapiro

FIG. 6. As in Fig. 3 but for $\chi = 1.25$.

for his helpful remarks. This research is supported through the National Science Foundation Grant ATM-8815008.

APPENDIX

Estimating the PV Destruction Rate

The PV destruction rate in WEM is approximated as follows (note that the parameters and variables described in this appendix are defined in the same way as in WEM).

Supposing that the upper-layer vortex patch covers an area A_1 , the outward mass flux can also be represented as

$$F_{\text{out}} = \rho_1 D_1 \frac{dA_1}{dt}.$$

From (3.12) and (3.13) of WEM, we derive

$$\frac{dA_1}{dt} = \frac{2\pi\rho_s r_c c_D v_c^2}{\rho_1 f_0 D_1}. \quad (\text{A.1})$$

Because the divergent potential flow has no net effect on the absolute circulation bounding the upper-layer vortex patch, the upper-layer absolute circulation is conserved; that is,

$$\frac{dC_1}{dt} = \eta_1 \frac{dA_1}{dt} + A_1 \frac{d\eta_1}{dt} = 0, \quad (\text{A.2})$$

where C_1 is the absolute circulation surrounding the upper-layer vortex patch, and η_1 and A_1 represent the absolute vorticity and the area of the upper patch, respectively. Then from (A.1) and (A.2), we obtain

$$\frac{d\eta_1}{dt} = -\frac{2\pi\rho_s r_c c_D v_c^2 \eta_1}{\rho_1 f_0 D_1 A_1}.$$

Therefore, if we assume that the vertical potential temperature lapse rate is constant in time, a simple estimation of the PV change rate due to the absolute vorticity change would be

$$\frac{d(\text{PV})}{dt} \approx -g \frac{d\eta_1}{dt} \frac{\partial\theta}{\partial p} = g \frac{2\pi\rho_s r_c c_D v_c^2 \eta_1}{r_1 f_0 D_1 A_1} \frac{\partial\theta}{\partial p}. \quad (\text{A.3})$$

Calculating (A.3) with typical values of the parameters in the model (as used in WEM), we can estimate the PV change rate to be at most -1 PVU/day. (The maximum is estimated by using the initial model information, when the PV patch area A_1 is smallest, and by representing η_1 by an extreme value, f_0 .) This result suggests that this model does not overestimate the PV destruction rate in the upper troposphere due to the heating.

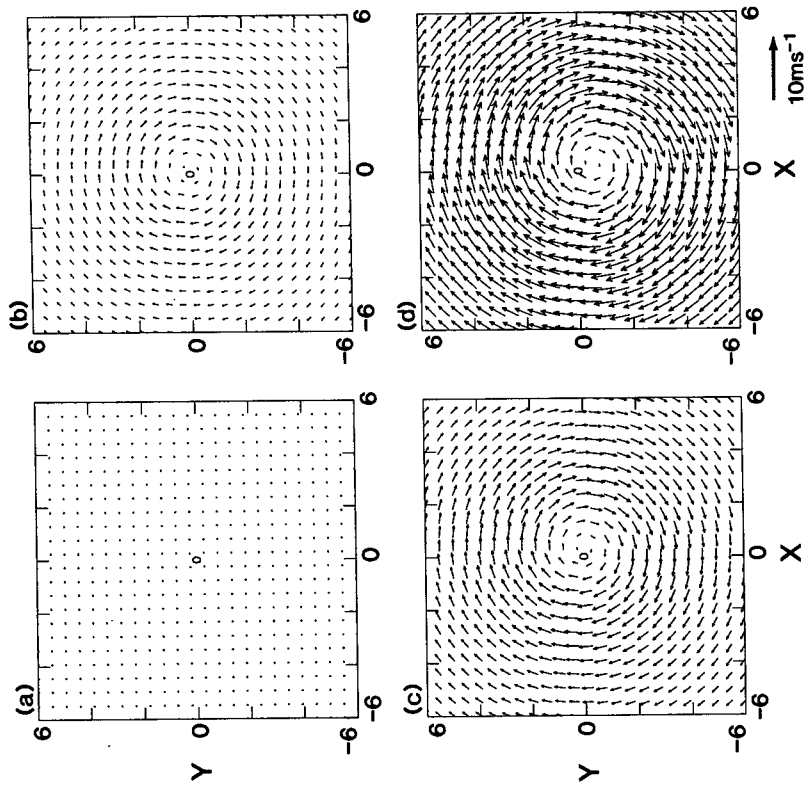


FIG. 8. As in Fig. 3 but for $\chi = 0.25$.

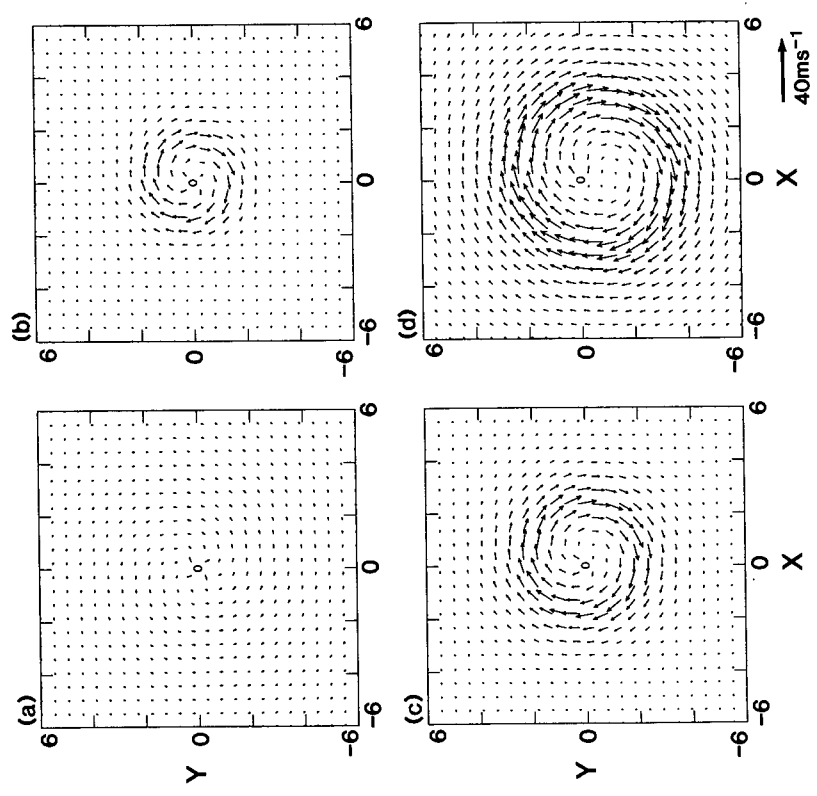


FIG. 7. As in Fig. 2 but for $\chi = 0.25$.

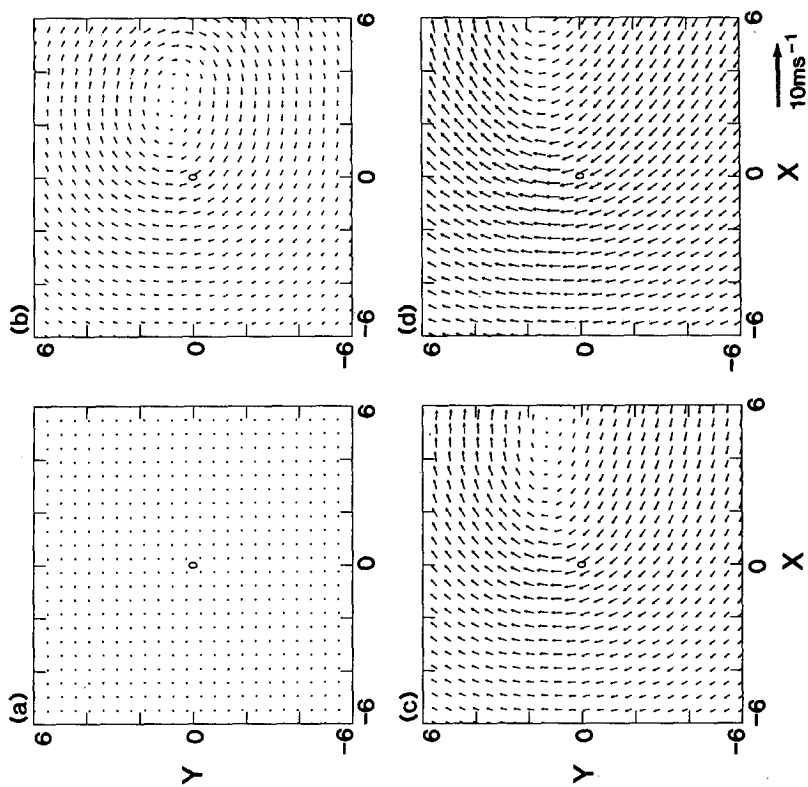


FIG. 9. As in Fig. 2 but for $\chi = 5$.

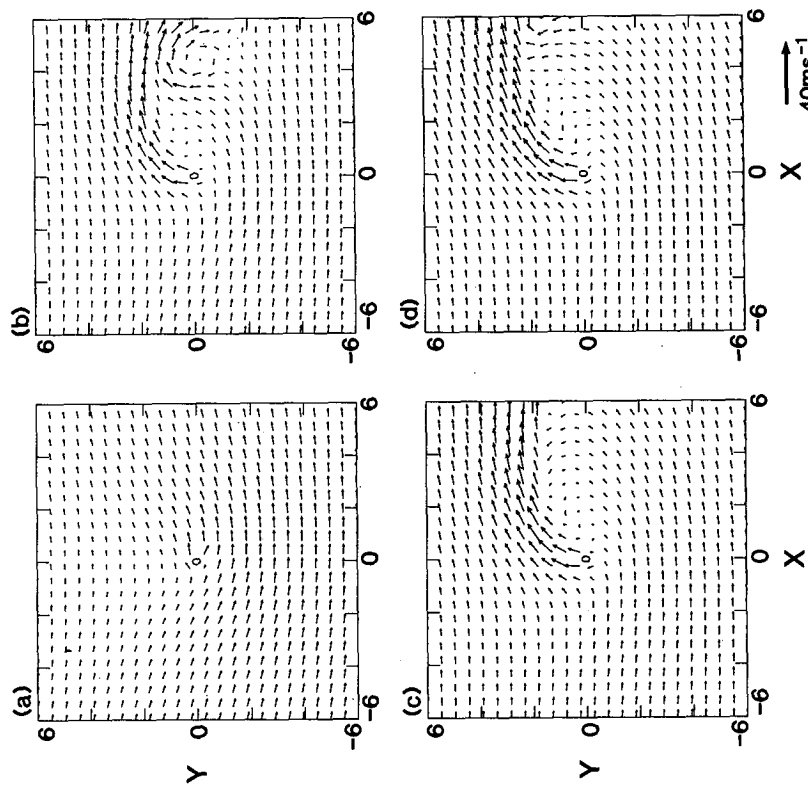


FIG. 10. As in Fig. 3 but for $\chi = 5$.

REFERENCES

- Anthes, R. A., 1972: Development of asymmetries in a three-dimensional numerical model of the tropical cyclone. *Mon. Wea. Rev.*, **100**, 461–476.
- Black, P. G., and R. A. Anthes, 1971: On the asymmetric structure of the tropical cyclone outflow layer. *J. Atmos. Sci.*, **28**, 1348–1366.
- Davis, C. A., and K. A. Emanuel, 1991: Potential vorticity diagnostics of cyclogenesis. *Mon. Wea. Rev.*, **119**, 1929–1953.
- Emanuel, K. A., 1986: An air–sea interaction theory for tropical cyclones. Part I: Steady-state maintenance. *J. Atmos. Sci.*, **43**, 585–604.
- Flatau, M., and D. E. Stevens, 1993: The role of outflow-layer instabilities in tropical cyclone motion. *J. Atmos. Sci.*, **50**, 1721–1733.
- Holland, G. J., and R. T. Merrill, 1984: On the dynamics of tropical cyclone structural changes. *Quart. J. Roy. Meteor. Soc.*, **110**, 723–745.
- Hoskins, B. J., M. E. McIntyre, and A. W. Robertson, 1985: On the use and significance of isentropic potential-vorticity maps. *Quart. J. Roy. Meteor. Soc.*, **111**, 877–946.
- Kurihara, Y., and R. E. Tuleya, 1974: Structure of a tropical cyclone developed in a three-dimensional numerical simulation model. *J. Atmos. Sci.*, **31**, 893–919.
- Langford, J. S., and K. A. Emanuel, 1993: An unmanned aircraft for dropwindsonde development and hurricane reconnaissance. *Bull. Amer. Meteor. Soc.*, **74**, 367–375.
- Merrill, R. T., 1988: Characteristics of the upper-tropospheric environmental flow around hurricanes. *J. Atmos. Sci.*, **45**, 1665–1677.
- Molinari, J., 1993: Environmental controls on eye wall cycles and intensity change in Hurricane Allen (1980). *Proc. ICSU/WMO Int. Symp. on Tropical Cyclone Disasters*, Beijing, China, World Meteorological Society, Peiking University Press, 328–337.
- Ooyama, K. V., 1987: Numerical experiments of steady and transient jets with a simple model of the hurricane outflow layer. Preprint, *17th Conf. on Hurricanes and Tropical Meteorology*, Miami, Florida, Amer. Meteor. Soc., 318–320.
- Rotunno, R., and K. A. Emanuel, 1987: An air–sea interaction theory for tropical cyclones: Part II. *J. Atmos. Sci.*, **44**, 542–561.
- Shapiro, L. J., 1992: Hurricane vortex motion and evolution in a three-layer model. *J. Atmos. Sci.*, **49**, 140–153.
- Wu, C.-C., and K. A. Emanuel, 1993: Interaction of a baroclinic vortex with background shear: Application to hurricane movement. *J. Atmos. Sci.*, **50**, 62–76.